Biogeosciences Discuss., 10, 1747–1791, 2013
www.biogeosciences-discuss.net/10/1747/2013/
doi:10.5194/bgd-10-1747-2013

Biogeosciences Discussions
Open Access

Pan-Arctic linkages between snow accumulation and growing season air temperature, soil moisture and vegetation

K. A. Luus[1,2], **Y. Gel**[3], **J. C. Lin**[1,4], **R. E. J. Kelly**[2], **and C. R. Duguay**[2]

[1]Earth and Environmental Sciences, University of Waterloo, Waterloo, ON, Canada
[2]Geography and Environmental Management, University of Waterloo, Waterloo, ON, Canada
[3]Statistics and Actuarial Science, University of Waterloo, Waterloo, ON, Canada
[4]Atmospheric Sciences, University of Utah, Salt Lake City, UT, USA

Received: 20 December 2012 – Accepted: 18 January 2013 – Published: 31 January 2013

Correspondence to: K. A. Luus (kaluus@uwaterloo.ca)

Published by Copernicus Publications on behalf of the European Geosciences Union.

Abstract

Arctic field studies have indicated that the air temperature, soil moisture and vegetation at a site influence the quantity of snow accumulated, and that snow accumulation can alter growing season soil moisture and vegetation. Climate change is predicted to bring about warmer air temperatures, greater snow accumulation and northward movements of the shrub and tree lines. Understanding the response of northern environments to changes in snow and growing season land surface characteristics requires: (1) insights into the present-day linkages between snow and growing season land surface characteristics; and (2) the ability to continue to monitor these associations over time across the vast pan-Arctic. The objective of this study was therefore to examine the pan-Arctic (north of 60° N) linkages between two temporally distinct data products created from AMSR-E satellite passive microwave observations: GlobSnow snow water equivalent, and NTSG (growing season air temperature, soil moisture and vegetation transmissivity). Due to the complex and interconnected nature of processes determining snow and growing season land surface characteristics, these associations were analyzed using the modern non-parametric technique of Alternating Conditional Expectations (ACE), as this approach does not impose a predefined analytic form. Findings indicate that regions with lower vegetation transmissivity (more biomass) at the start and end of the growing season tend to accumulate less snow at the start and end of the snow season, possibly due to interception and shading. Warmer air temperatures at the start and end of the growing season were associated with diminished snow accumulation at the start and end of the snow season. High latitude sites with warmer mean annual growing season temperatures tended to accumulate more snow, probably due to the greater availability of water vapor for snow season precipitation at warmer locations. Regions with drier soils preceding snow onset tended to accumulate greater quantities of snow, likely because drier soils freeze faster and more thoroughly than wetter soils. Understanding and continuing to monitor these linkages at the regional scale using the ACE approach can allow insights to be gained into the complex response of Arctic

BGD
10, 1747–1791, 2013

ecosystems to climate-driven shifts in air temperature, vegetation, soil moisture and snow accumulation.

1 Introduction

Interactions between cryospheric, biological and atmospheric components play an important role in the Arctic climate system (Serreze and Barry, 2005), and linkages between snow water equivalent (SWE), soil moisture, air temperature and the quantity of vegetation determine the carbon balance of northern regions (Sitch et al., 2007). Northern field studies have determined that snow accumulation is influenced by the snow season climate (Sturm et al., 1995), and that the presence of vegetation increases snow accumulation near shrubs due to wind trapping (Sturm et al., 2001a) while regions with greater quantities of evergreen biomass tend to retain less snow due to interception and sublimation (Pomeroy et al., 2002). Changes in snow accumulation have also been found to alter vegetation species composition at an Arctic tundra site (Wahren et al., 2005), and have been found to result in anomalous soil moisture values over the following growing season in a semiarid area of Eurasia (Shinoda, 2001). However, due to the heterogeneity displayed by northern regions as well as the scale dependence of many environmental processes, feedbacks and interactions, the pan-Arctic linkages between snow and growing season land surface properties have not previously been well understood.

A systematic pan-Arctic analysis of these associations over annual and seasonal timescales, and how they vary across vegetation classes, can therefore provide important insights into feedbacks and spatial linkages between snow season and growing season land surface characteristics. Due to the lack of exhaustive coverage by ground-based sampling, understanding the complex response of pan-Arctic environments to climate change relies on the ability to characterize land surface properties using remote sensing observations, and to analyze shifts in the associations between snow and growing properties at the regional to circumpolar resolution. The passive

BGD
10, 1747–1791, 2013

microwave data products analyzed in this study were created by researchers at the Finnish Meteorological Institute (FMI) (e.g. Luojus et al., 2009) and the University of Montana's Numerical Terradynamic Simulation Group (NTSG) (e.g. Jones and Kimball, 2012) from Advanced Microwave Scanning Radiometer for the Earth Observing System (AMSR-E) observations. The FMI group produced GlobSnow SWE, and the NTSG group produced growing season estimates of air temperature, soil moisture, vegetation transmissivity and fractional water content. A comprehensive summary of these datasets can be found in Appendix A.

The objective of this study was to analyze linkages between GlobSnow SWE and NTSG growing season air temperature, soil moisture and vegetation transmissivity for the entire terrestrial region north of 60° N. The aims were to examine: (1) similarities in general tendencies of the land surface between seasons (e.g. do regions that have greater quantities of vegetation also tend to have more SWE?); (2) whether regions that experience certain conditions at the end of the growing season tend to receive altered quantities of SWE (e.g. do areas that tend to be warmer at the end of the growing season tend to accumulate less snow in the early portion of the snow season?); and (3) associations between snow accumulation at the end of the snow season and land surface variables at the start of the growing season (e.g. do sites with slower snowmelt at the end of the snow season tend to have drier soil moisture at the start of the growing season?).

The modern nonparametric approach of Alternating Conditional Expectations (ACE) was applied to analyze the relationships between each pair of snow and growing season variables from passive microwave observations. As the ACE technique has not yet been widely used in the biogeosciences, a thorough explanation of the theory behind ACE and the strategies used to assess ACE output are provided below. Findings indicated that the linkages and thresholds found between snow accumulation and growing season variables (air temperature, soil moisture and vegetation) at a coarse (25 km) resolution corresponded well with in situ findings of site-level linkages and thresholds, despite the scale dependence and ecological heterogeneity of Arctic regions. Further

BGD
10, 1747–1791, 2013

monitoring of these associations at a variety of scales using the ACE approach is therefore recommended in order to gain insights into the response of Arctic ecosystems to climate change.

2 Alternating conditional expectations (ACE)

The ACE approach can be used to describe the underlying, non-linear relationships that exist between predictor and response variables (Breiman and Friedman, 1985; Frank and Lanteri, 1988). Previous work has indicated that the ACE technique can be used to reveal complex relationships that exist in large datasets (e.g. Gel, 2007).

A standard linear regression approach provides a least squares estimate of the relationship between a response variable (y) and one or more predictor variables (x_j) according to regression coefficients (a_j) and an intercept (a_0):

$$y = a_0 + \sum_{j=1}^{p} a_j x_j \tag{1}$$

The ACE approach instead describes the non-linear relationships between y and x_j by identifying the least squares optimal smoothing functions g and f_j that effectively "linearize" the association between $g(y)$ and $f_j(x_j)$:

$$g(y) = \sum_{j=1}^{p} f_j(x_j) \tag{2}$$

These optimal smoothing functions g and f_j are identified by minimizing the error function

$$e^2(g, f_1, \ldots f_p) = E\left[g(y) - \sum_{j}^{p} f_j(x_j)\right]^2 \tag{3}$$

BGD
10, 1747–1791, 2013

through an iterative two-loop process for p predictors. The ACE algorithm uses initial values of $g(y) = \frac{y}{\|y\|}$ and $f_j(x_j) = b_j x_j, j = 1,p$, where $\|.\| = \sqrt{[E(.)^2]}$, and b_j are coefficients estimated through ordinary least squares regression. A loop is then used to optimize the predictor transformation function:

$$f_j^{k+1}(x_j) = E\left[g^k(y) - \sum_{i \neq j} f_i^k(x_i)|x_j\right] \quad (4)$$

Once ϵ^2 fails to decrease, the response transformation function $g(y)$ is then optimized in an outer loop using the final values of $f_j(x_j)$

$$g^{k+1}(y) = \frac{E\left[\sum_j f_j^k(x_j)|y\right]}{\left|\left|E\left[\sum_j f_j^k(x_j)|y\right]\right|\right|} \quad (5)$$

until ϵ^2 again fails to decrease (Breiman and Friedman, 1985; Frank and Lanteri, 1988).

Proof exists that the ACE algorithm results in convergence of f_j and g to their optimal transformations, which need not be either of a specific analytic form or monotonic (Breiman and Friedman, 1985; Frank and Lanteri, 1988). The resulting output is therefore expressed according to the point pairs $[x_j, f_j(x_j)]$ and $[y, g(y)]$, rather than by a specific mathematical form. Visual analysis consists of examining scatter plots of these point pairs, where each plot indicates the original data values (e.g. y and x_1) relative to their transformed values (e.g. $g(y)$ and $f_1(x_1)$) (Frank and Lanteri, 1988). Since the ACE technique finds the least squares optimal values of g and f_j such that the linear association between $g(y)$ and $\sum_{j=1}^{p} f_j(x_j)$ is maximized, it is crucial that the plots of point pairs $[x_j, f_j(x_j)]$ and $[y, g(y)]$ be interpreted relative to one another.

In order to demonstrate how the output from ACE is analyzed, a very simple example is provided in Fig. 1a, b. In this example, the health of two hypothetical plants

BGD
10, 1747–1791, 2013

is observed at varying levels of soil moisture. The black plant reaches peak health at intermediate levels of soil moisture (0.25) but its health is diminished at greater levels of soil moisture, whereas the green plant requires greater soil moisture for peak health (0.35) and is more resilient under very wet conditions. If a linear regression approach was used to assess the strength of these relationships, findings may indicate that the association between health and soil moisture is stronger for the green plant ($R^2 = 0.89$) than for the black plant ($R^2 = 0.03$). A non-linear transformation of x_j could then be manually selected and applied prior to rerunning the linear regression. However, this option is not feasible when the associations are more complex or the best possible fit may not be of a known analytic form. The ACE approach instead identifies the optimal non-linear transformations $g(y)$ and $f_1(x_1)$, which are plotted as point pairs $[x_1, f_1(x_1)]$ and $[y, g(y)]$ in Fig. 1a, b.

The ACE transformation applied to soil moisture of the green plant ($f_{\text{green}}(x_{\text{green}})$) appears approximately logarithmic relative to the observed values of soil moisture (x_{green}), and seems to plateau at soil moisture values of approximately 0.4 (Fig. 1a, b). Since the transformation applied to vegetation health ($g_{\text{green}}(y_{\text{green}})$) was approximately linear and monotonic with respect to health (y_{green}), these plots can be understood as indicating that the positive response of vegetation health of the green plant to increasing levels of soil moisture is strongest at low levels of soil moisture (0–0.35). For the black plant, the plot of soil moisture (x_{black}) versus transformed values of soil moisture ($f_{\text{black}}(x_{\text{black}})$) has a parabolic shape, with a vertex in the transformed values of soil moisture at values of 0.25. As the transformation applied to health of the black plant ($g_{\text{black}}(y_{\text{black}})$) is linear and monotonic with respect to vegetation health (y_{black}), it can be concluded that greater soil moisture is associated with improved vegetation health of the black plant at soil moisture values of 0–0.25, and associated with diminished vegetation health at soil moisture values of 0.25–0.5.

The ACE approach has therefore uncovered strong, non-linear associations between vegetation health and soil moisture for both the green ($R^2 = 0.95$) and black ($R^2 = 0.87$) plants, and has indicated the shape of these relationships. The values of predictor and

BGD
10, 1747–1791, 2013

response variables were specifically selected in this example such that the associations between x_j and y could be easily evaluated from plots of $[x_j, y]$, and that the correspondence between these plots and the values shown in plots of point pairs $[x_j, f_j(x_j)]$ and $[y, g(y)]$ was easily understood. However, when the ACE approach is applied to assess complex associations in large datasets, the shape and strength of associations shown in plots of $[x_j, f_j(x_j)]$ and $[y, g(y)]$ cannot be visually interpreted from plots of $[x_j, y]$. As a result, valuable insights into both the shape and strength of the associations between GlobSnow SWE and NTSG growing season land surface variables can be gained through application of the ACE technique.

3 Methodology

GlobSnow SWE and NTSG growing season land surface variables were first prepared for analysis and partitioned into vegetation classes. An exploratory analysis was then conducted to examine the potential spatial relationships between datasets. Results from the preliminary analysis indicated that the modern nonparametric method of Alternating Conditional Expectations (ACE) was well suited for the analysis of pairwise linkages between GlobSnow SWE and NTSG growing season land surface datasets. The ACE technique was therefore applied to examine pan-Arctic linkages between SWE and growing season air temperature, soil moisture and vegetation transmissivity.

3.1 Data preparation

Preliminary data processing consisted of identifying the start and end dates of the snow season and growing season independently for each 25 km pixel, and each year (2003–2008) as defined by the NTSG and GlobSnow products. Observations from the NTSG product were only used during the period of time when the ground was unfrozen and snow-free according to both the NTSG and GlobSnow products. Conversely, the GlobSnow observations of SWE were only used for the period of time when the ground

BGD
10, 1747–1791, 2013

was frozen and dry snow was present, ranging from the date in autumn when SWE > 0 mm was first observed up until the date in spring when the last observation of SWE > 0 mm was recorded. The mean annual (2003–2008) values could therefore be calculated, along with mean values for the first thirty days and last thirty days of the snow and growing seasons for each year. As the GlobSnow version 0.9.1 product sets SWE to 0 mm on days where wet snow is observed, smaller values of SWE at the start or end of the snow season are indicative of less snow accumulation or more gradual snow onset/melt. Regions with fractional water content > 0.5 were masked out of analysis.

3.2 Vegetation classes

As vegetation classes are often used to describe snow and growing season characteristics of the land surface, associations between snow and growing season variables were analyzed within seven Arctic vegetation classes defined using two well established categorizations: the SYNMAP (Jung et al., 2006) and the Circumpolar Arctic Vegetation Map (CAVM) (Walker et al., 2005). As CAVM is only available north of the treeline, SYNMAP was first used to classify the entire pan-Arctic, but was substituted with CAVM categorizations where available. The resulting 67 classes were then reorganized into seven vegetation classes shown in Table 1.

In order for the analysis to proceed, it was important to first ensure that the aforementioned vegetation classes represent distinct populations of SWE, soil moisture, air temperature and vegetation transmissivity, and that the interannual variability of each land surface characteristic was small enough that mean 2003–2008 values could be analyzed. Furthermore, it was important to assess whether the vegetation classes represented distinct populations of vegetation net primary productivity.

Analysis of the heterogeneity of distributions of AMSR-E derived variables and NPP were assessed between years and between vegetation classes using Levene's test (Levene, 1960). Levene's test was selected because it provides an assessment of the deviation of an observation from a group mean, is robust to non-normality, and has

BGD
10, 1747–1791, 2013

been used for a variety of scientific applications, including environmental sciences (Gatswirth et al., 2009). Findings indicated that heterogeneity of variances existed across vegetation classes (p-value $< 10^{-5}$) (Table 2), and that homogeneity of variances existed between years ($0.5 \leq p$-value ≤ 0.99). Analysis could therefore proceed by aggregating mean 2003–2008 values, and by assessing linkages separately for each vegetation class.

3.3 Exploratory analysis

A brief exploratory analysis of mean values for each variable over the 2003–2008 time period (Fig. 2a–f) indicated that growing season air temperature and vegetation opacity display a latitudinal gradient, with cooler temperatures and less vegetation at high latitudes, likely due to the temperature dependence of Arctic vegetation (Hare, 1968; Ritchie and Hare, 1971). Soil moisture and snow water equivalent show greater spatial variability due to topographic, meteorological, atmospheric, and land surface influences (Callaghan et al., 2011; Serreze and Barry, 2005). The distributions of mean 1982–2000 net primary productivity (in grams of carbon $m^{-2} y^{-1}$) from the Global Production Efficiency Model (GloPEM) (Prince and Goward, 1995) appear to correspond with the spatial patterns of vegetation classes selected for this study.

Greater values of SWE occur in regions where more snowfall occurs, where windblown snow is accumulated, or where snowmelt during the snow season is less frequent or less substantial. Ideally, these contributions to SWE could be partitioned so that the linkages between growing season variables with snowfall, snowmelt and windblown snow deposition could be analyzed; however, current estimates of precipitation are presently unreliable at high latitudes, especially during the snow season, and the amount of snow must therefore be examined in terms of SWE alone. It is important to note that mean values of SWE at the start and end of the snow season are thus indicative of both accumulation as well as the speed of snow onset/melt. At the start and end of the snow season, mean values of SWE are greater at sites where snowmelt and snow accumulation occur more rapidly, as these have fewer days with low reported

BGD
10, 1747–1791, 2013

values of SWE. Similarly, low values of SWE at the start or end of the snow season are indicative of less snow accumulation, or slower snow onset or melt.

3.4 Preliminary regression analysis

Preliminary regression analysis consisted of applying linear regression and principal component analysis (PCA) to assess the possibility of linear relationships between snow and growing season values. However, it is likely that the assumption of linearity cannot be fulfilled, and in addition, application of the Shapiro-Wilk test (D'Agostino and Stephens, 1986) indicated that the soil moisture and air temperature datasets had non-normal distributions at high latitudes (p-values < 0.01). Linear regression and PCA therefore do not represent suitable techniques for examining associations between the GlobSnow SWE and NTSG land surface variable datasets, but the findings from these approaches are of interest because PCA and linear regression are widely used to examine environmental linkages. The derived R^2 from classical single and multiple linear regressions (Table 3) along with the multiple linear regression of SWE vs factor scores obtained from the principal component analysis (PCA) of air temperature (TA), volumetric soil moisture (MV), and vegetation canopy transmissivity (TC) (Table 4) indicated that the linear associations between SWE and growing season variables were very weak or non-existent.

Conversely, a multivariate ACE analysis of these associations yielded much greater R^2 values for every vegetation class and time period relative to the linear regression (Table 5), while a univariate ACE analysis indicated highly significant (p-value $< 10^{-5}$) pairwise associations for all vegetation classes, variables and time periods. Moreover, the p-values of all coefficients in multivariate ACE analysis were also highly statistically significant. As a result, we can conclude that there exist no collinearities in the non-parametrically transformed growing season variables. The findings from this stage of preliminary regression analysis strongly support the employment of the non-parametric ACE technique to explore the non-linear associations within this dataset.

BGD
10, 1747–1791, 2013

3.5 ACE

The ACE approach was applied to determine the strength and directionality of the associations between SWE and growing season values for each vegetation class and time period separately. Associations between these datasets could therefore be examined despite their lack of temporal overlap by comparing: (1) mean annual values; (2) associations between the mean values of SWE over the last thirty days of the snow season with mean land surface values over the first thirty days of the snow season before snowmelt; (3) associations between the mean land surface variables over the last thirty days of the growing season with mean values of SWE occurring after the first observation of dry snow on frozen ground. These time periods are referred to as "mean", "spring" and "autumn", respectively, throughout the paper.

4 Results and discussion

Findings from the ACE analysis of associations between SWE, air temperature, soil moisture and vegetation transmissivity are presented and discussed below in relation to in situ observations. The results have been divided into separate sections according to the growing season values associated with SWE, with subsections corresponding to different time periods. Each section contains tables showing the strength of associations (R^2 values) of ACE transformed SWE and growing season values (Table 5), and plots indicating the optimal transformations of SWE and growing season values according to the seven vegetation classes (Figs. 3a–g, 4a–g and 5a–g).

4.1 Air temperature and SWE

At tundra sites, a positive, non-linear association exists between mean annual SWE and mean growing season temperatures such that sites which tend to be slightly warmer tend to accumulate more snow than cooler sites (ACE $R^2 = 0.20$–0.38). Yet,

BGD
10, 1747–1791, 2013

sites that tend to be warmer at the start and end of the growing season tend to contain less snow during initial snow onset and final snow melt each year.

4.1.1 North of the treeline, greater mean annual SWE with warmer growing seasons

The associations between mean 2003–2008 SWE and growing season air temperature at tundra sites are non-linear. As a result, findings from the linear regression approach indicate weaker associations at tundra sites (R^2 = 0.04–0.20) (Table 3) than detected by the ACE transformations (R^2 = 0.20–0.38) (Table 5). The associations between growing season air temperature and SWE are weaker over forested regions, likely due to seasonal discrepancies in the mean growing season and mean snow season air temperatures (Overland et al., 1997; Rigor et al., 2000; Adams et al., 2000; Serreze and Barry, 2005). The following analysis therefore focuses mainly on the associations observed north of the treeline, although all plots can be found in Fig. 3a–g.

Examinations of Fig. 3e–g indicate sharp, positive transformations applied to low values of SWE (< 75 mm. Likewise, these plots show that the positive association between air temperature and SWE at these locations exists for sites with a mean annual growing season temperature of < 10 °C. Analysis of the ACE transformations provides an important source of information for understanding these linkages. Arctic tundra regions are characterized by very cold temperatures during the snow season that limit the availability of water vapor and the rate of precipitation (Bonan, 2002; Serreze and Barry, 2005), thereby resulting in diminished accumulation of snow, and it is likely that the influence of diminished water vapor explains the association between SWE and growing season air temperature. Analysis of the ACE transformations therefore indicates that in tundra regions with < 75 mm of SWE and mean growing season temperatures of 0–10 °C, sites that tend to have slightly warmer air temperatures will likely tend to accumulate greater quantities of SWE.

BGD
10, 1747–1791, 2013

4.1.2 Warmer spring/autumn temperatures and less SWE

ACE analysis indicated that weak, approximately linear associations exist between warmer air temperatures and diminished SWE at the start and end of the snow season (Table 5). Regions that tended to be warmer at the start and end of the snow season therefore tended to have less SWE at the start and end of the snow season, or more gradual snow onset or melt.

The associations between autumn SWE and air temperature were found to be of weak to moderate strength in forested regions (ACE $R^2 = 0.14–0.25$). Weak associations were observed in tundra regions (ACE $R^2 = 0.06–0.10$). As forest soils have been observed to be warmer and to freeze more gradually than tundra soils at the start of the snow season (Rouse, 1984; Smith et al., 1998), it is likely that the influence of antecedent growing season temperatures on the capacity of a dry snowpack to develop at the start of the snow season would be stronger over regions without permafrost.

Whereas the associations between SWE and air temperature are strongest in autumn over forested regions, these associations are of weak to moderate strength in spring at sites north of the treeline (ACE $R^2 = 0.12–0.17$), and are weaker over forested regions (ACE $R^2 = 0.04–0.15$) (Table 5). High latitude Arctic sites undergo rapid snowmelt due to the low albedo and low shading of Arctic vegetation, and similarity in the timing of the summer equinox and date of snowmelt (Bonan, 2002). As these effects are stronger at high latitude sites, it is reasonable that the most rapid snowmelt would be observed in regions north of the treeline. Furthermore, as air temperatures similarly show a strong gradient (Fig. 2a–f), it is reasonable that the regions in which snowmelt occurred most rapidly would also be those in which air temperatures following snowmelt were coolest.

4.2 Soil moisture and SWE

Although the ACE transformed associations between mean annual SWE and mean growing season soil moisture are weak across all vegetation classes (0.02–0.09)

BGD
10, 1747–1791, 2013

(Table 5), an examination of the shape of these non-linear associations indicates a positive association between mean annual SWE and soil moisture at sites with very low SWE (< 90 mm) and low soil moisture (< 0.17), with thresholds that correspond with in situ observations. The seasonal associations between SWE and soil moisture are complex, resulting in deeper freezing and faster runoff on drier soils, such that an inverse association exists between SWE and soil moisture in spring and autumn (Fig. 4a–g).

4.2.1 Mean annual SWE and soil moisture

The relationships between mean annual SWE and soil moisture are weak, non-linear, and vary according to vegetation class over which they are examined. Seasonal differences in precipitation patterns (Serreze and Barry, 2005), as well as confounding factors such as soil freeze patterns, vegetation (Hardy et al., 2001; Johnsson and Lundin, 1991), ponds (French and Binley, 2004), topography (Burt and Butcher, 1985) and soil type (Janowicz et al., 2003; Williams and Ratsetter, 1999) are likely to limit the strength of the associations between SWE and soil moisture, and limit the extent to which these associations can be regionally generalized. Nevertheless, the ACE transformations indicate that positive associations exist between mean annual SWE and soil moisture in forested and barren regions that accumulate little snow (SWE < 90 mm) and have low soil moisture (< 0.17). Similarly, a positive association between soil moisture and SWE is observed over shrub dominated regions for all values of SWE and soil moisture, and over mixed forest regions accumulating less than 100 mm of SWE.

The influence of very low SWE (< 100 mm) has been studied in situ at barren (Ayres et al., 2010) and hardwood (Hardy et al., 2001) sites. Findings indicated that snow removal at the hardwood site resulted in greater soil heat loss, and therefore increased the proportion of ice in soil. As a result, snowmelt infiltration and soil moisture were reduced in plots where snow was removed (Hardy et al., 2001). Similarly, experimental manipulation of snow accumulation at a polar desert indicated that sites where greater quantities of snow were accumulated tended to have greater levels of soil moisture during the following growing seasons relative to paired control sites (Ayres et al., 2010). In

BGD
10, 1747–1791, 2013

the previously described experimental plots simulating low snow conditions, the barren site accumulated 10–50 mm of SWE and the hardwood site accumulated 80–100 mm of SWE. As a result, these studies indicated that diminished SWE led to diminished soil moisture in barren and hardwood plots with < 100 mm of SWE. Therefore, although the R^2 values from this study indicate that a weak and non-linear association exists between SWE and soil moisture across all vegetation classes, the ACE approach has elucidated similar thresholds and linkages as those which have been recorded in situ.

The ACE approach also indicated that a greater mean annual SWE is associated with greater soil moisture across all values observed over shrub dominated regions, and at low (< 0.15) levels of soil moisture in evergreen forests and graminoid tundra. Similarly, in a study conducted at the regional scale, anomalies in maximum annual snow depth and soil moisture were found to be associated in a semiarid region of Eurasia north of the Caspian-Aral seas (Shinoda, 2001). This region has maximum annual values of < 150 mm of SWE, and is classified as evergreen and deciduous forest in the present study. In years where snow accumulation tended to be greater, snowmelt onset was found to occur later and larger values of soil moisture were observed during the following growing season. The finding by Shinoda (2001) that SWE and soil moisture tend to be associated over semiarid evergreen regions is therefore consistent with findings from this study, which indicate positive associations between mean annual SWE and soil moisture at sites that tend to receive less mean annual SWE and tend to have low soil moisture.

4.2.2 SWE and soil moisture in spring and autumn

The associations between soil moisture and SWE are weak when examined over thirty day time periods in spring (ACE R^2 = 0.02–0.17) and autumn (ACE R^2 = 0.06–0.12). At mixed forest and deciduous sites, ACE transformations indicates that a positive association exists between spring soil moisture and SWE at sites with low (< 75 mm) snow accumulation. Similarly, results from a snow depth manipulation experiment conducted

BGD
10, 1747–1791, 2013

in a hardwood forest indicated diminished soil moisture following snowmelt in a hardwood forest with very low snow accumulation (Hardy et al., 2001).

The associations between SWE and soil moisture over remaining vegetation classes and time periods are slightly more complex. Although snow accounts for a large portion of annual precipitation, little of the moisture released through snowmelt in the Arctic is retained by soil (Willis et al., 1961) due to rapid snowemlt, runoff and outflow (Hardy et al., 2001; Johnsson and Lundin, 1991). For example, in a study at the Imnaviat Creek Arctic headwater, snow accumulation in spring accounted for 28–40 % of annual precipitation, only 10–19 % of the liquid water arising from snowmelt was stored in the active layer (Kane et al., 1991). Regions with greater accumulation of snow tend to contribute a larger percentage of snowmelt to runoff (Willis et al., 1961; Staple et al., 1960). It is therefore less likely that a positive association would be observed between SWE and soil moisture in spring and autumn in areas underlain by permafrost.

An inverse relationship is observed to exist between soil moisture at the end of the growing season, and the accumulation of SWE at the start of the snow season for all vegetation classes (Fig. 4a–g). Soil freezing occurs more slowly over wet soils than dry soils due to the influence of moisture on soil heat capacity (Willis et al., 1961; Hardy et al., 2001). As snow can only accumulate over cool soil surfaces, it is reasonable that soils which cool more rapidly at the start of the snow season may undergo greater net snow accumulation after freezing than warmer, wetter soils.

Likewise, in spring, an inverse association between soil moisture and SWE was observed over evergreen, shrub, tundra and barren regions with low (< 0.1) soil moisture (Fig. 4a–g). The portion of snowmelt that infiltrates into the soil surface relies on the rate of snow melt, soil water, soil frost and soil drainage (Hardy et al., 2001; Johnsson and Lundin, 1991). An inverse association therefore exists between seasonal infiltration and soil moisture levels during snowmelt (Zhao and Gray, 1999). The soil frost and soil drainage patterns at the end of the snow season can also be influenced by the levels of soil moisture observed prior to soil surface freezing at the start of the snow season (Hardy et al., 2001; Suzuki et al., 2006). Soils which are drier at the start of the

BGD
10, 1747–1791, 2013

snow season freeze more deeply than wetter soils and also thaw out more gradually (Willis et al., 1961). Furthermore, soils with frozen upper layers have diminished infiltration due to the influence of ice on reducing soil pore size and permeability (Zhao and Gray, 1999). Therefore, since drier soils tend to freeze faster and more deeply than wet soils, more opportunity exists for snow accumulation to occur at the start and end of the snow season over dry soils because melt is less likely to occur. Soils which are more thoroughly frozen throughout the snow season are likely to receive less infiltration of snowmelt, and are therefore likely to be drier at the start of the growing season.

4.3 Vegetation transmissivity and SWE

Mean annual SWE and vegetation transmissivity generally have a negative association north of the treeline, indicating greater SWE accumulation in regions with greater surface roughness or aboveground biomass (Fig. 5a–g). Conversely, the association between SWE and vegetation transmissivity in forested regions tends to be positive, such that SWE accumulation is limited in areas with greater aboveground biomass. At the start and end of the snow season, vegetation transmissivity is positively associated with SWE, which indicates more rapid melt or less snow accumulation at the start and end of the snow season in regions with more vegetation.

4.3.1 Mean annual SWE and vegetation transmissivity

The association between mean annual SWE and mean vegetation transmissivity (2003–2008) varies according to the predominant land cover, as well as the quantity of SWE received. In Arctic regions north of the treeline with a mean SWE accumulation of < 75 mm, an inverse association exists between vegetation transmissivity and SWE, indicating that locations with slightly more vegetation received much more snow annually than regions with diminished surface roughness and vegetation. Due to the non-linearity of the association between mean annual SWE and vegetation transmissivity over tundra and barren sites, the ACE transformation is useful in indicating that an

BGD
10, 1747–1791, 2013

association of moderate strength exists (R^2 = 0.19–0.29) whereas a linear regression may have indicated a weaker value for these same values (R^2 = 0.06–0.15) without elucidating the shape of this association (Table 5).

The association between vegetation biomass and SWE may be due in part to the influence of local precipitation on vegetation species compositions, which has previously been observed over the Brooks Range of Alaska by Evans et al. (1989). In northern regions, the health and productivity of vegetation can be compromised by very cold air, low soil temperatures and rain-on-snow events. Snow has been observed to provide vegetation with insulation from cold soil temperatures, and protection from dehydration, frost damage and high winds (Wardle, 1968; Tranquillini, 1964). Therefore, where snow accumulation is more substantial and remains on the ground for a longer time in spring, higher NDVI values have been observed (Grippa et al., 2005), which indicate greater health or quantity of aboveground biomass (Jensen, 2007).

The observed patterns of snow and vegetation are likely also due to the dominant influence of vegetation biomass on trapping snow redistributed by wind (Essery and Pomeroy, 2004; Sturm et al., 2001a; Fitzgibbon and Dunne, 1979). Areas that tend to accumulate more snow also tend to accumulate greater quantities of windblown organic materials throughout the snow season (Walker et al., 2001), and undergo greater rates of organic matter decomposition throughout the snow season since they have warmer soil temperatures (Nowinski et al., 2010). Both of the aforementioned influences can lead to nutrient rich conditions in regions receiving greater accumulation of snow, which can create growing season conditions that are conducive to plant growth. It is therefore possible that greater quantities of snow and vegetation tend to be collocated in Arctic regions due to the influence of snow on encouraging plant growth, and the influence of vegetation on encouraging snow accumulation. Spatial variability may therefore also play a role in this association, as high Arctic regions both accumulate small quantities of snow and contain little aboveground biomass.

Findings from the ACE approach indicated an inverse association between vegetation biomass and SWE in shrub-dominated regions with a mean annual SWE of

BGD
10, 1747–1791, 2013

75–150 mm ($R^2 = 0.26$). Although shrub dominated regions trap snow more readily than regions which are more sparsely vegetated (Pomeroy et al., 1997; Sturm et al., 2001a,b; Liston and Sturm, 2002), the primary driver of snow accumulation in shrub-dominated regions is topography rather than the height or density of aboveground biomass. Snow accumulation at shrub-dominated sites is therefore greatest in the proximity of large, flat regions, and tends to be greater in flatter valleys than on hill slopes (Pomeroy et al., 1995, 2006; MacDonald et al., 2009). As vegetation transmissivity is a function of both canopy extinction and surface roughness (Njoku and Chan, 2005; Jones et al., 2010), and shrub-dominated sites south of the CAVM defined treeline are found in topographically varying landscapes (Fig. 2a–f), the positive association between vegetation transmissivity and SWE may be due to the increased accumulation of snow in regions that show diminished surface roughness at the 25 km scale.

The ACE analysis indicates that snow accumulation at low SWE (< 115 mm) evergreen forest sites is maximized when less vegetation is present ($R^2 = 0.10$). Likewise, field studies have found that snow accumulation is greater in clearings than coniferous forests (Golding and Swanson, 1986; Gelfan et al., 2004), since coniferous trees intercept snowfall, and have been observed to allow 20–50 % of precipitation to evaporate or sublimate Lundberg and Halldin (2001). However, although coniferous stands with dense crowns limit snow accumulation, sparser evergreen forests can encourage snow deposition (Church, 1933). Based on the findings from the ACE analysis, it appears that the effects of evergreen forests on limiting snow accumulation are strongest at low SWE (< 115 mm) sites, whereas at high SWE (>115 mm) sites, a slightly positive association appears to exist between vegetation biomass and SWE. It is reasonable that wind redistribution would be a dominant process when availability of fresh snow is great, but that sublimation, interception and melt would be dominant processes when snow accumulation is limited. However, further field investigations would be required to better elucidate these drivers and clarify the dependence of these associations on the stated thresholds.

BGD
10, 1747–1791, 2013

4.3.2 In spring and autumn, slower snowmelt in areas with more vegetation

Across all vegetation classes, positive associations of moderate strength exist between the mean values of SWE over the last thirty days of the snow season and the mean values of vegetation transmissivity over the first thirty days of the growing season (ACE $R^2 = 0.19–0.31$). The presence of this association indicates that regions with greater quantities of vegetation or greater surface roughness tend to contain a lower mean quantity of snow over the last thirty days of the snow season. This association is approximately linear across all vegetation classes (Fig. 5a–g).

Field studies have largely indicated that snow depletion occurs more gradually in regions with greater quantities of vegetation. The rates of snowmelt in boreal and taiga forests have been observed to diminish with increasing canopy density (Pomeroy et al., 1997; Metcalfe and Buttle, 1998; Gelfan et al., 2004). This effect is due to the influence of the forest canopy on limiting shortwave radiation received by snow, and its effect on slowing wind speeds, thereby limiting fluxes of latent and sensible heat (Metcalfe and Buttle, 1998). Similarly, Arctic sites with tall, thick-stemmed shrubs have been observed to undergo snowmelt more slowly than regions with shorter vegetation, as shorter plants remain buried within the snowpack at the end of the snow season, resulting in greater albedo and less absorption of solar radiation (Sturm et al., 2005).

When examining vegetation transmissivity over the last thirty days of the growing season against SWE over the first thirty days of the snow season, a positive, approximately linear association of moderate strength can be identified for all sites south of the treeline (ACE $R^2 = 0.17–0.30$). Forested sites containing greater quantities of aboveground biomass therefore tend to accumulate less snow over the first thirty days following the date of initial snowfall than sites with less biomass. Field studies have indicated that interception and sublimation by dense canopies diminish snow accumulation (Pomeroy et al., 1999, 2002; Lundberg and Halldin, 2001), and it is likely that these processes likewise limit initial snow accumulation over regions containing greater densities of shrubs or mixed forest vegetation. The observed associations between

BGD
10, 1747–1791, 2013

SWE and vegetation biomass over tundra and barren regions appear weak but positive. However, to date, field studies have focused mainly on characterizing the influence of vegetation on mean annual snow accumulation, and on the magnitude and timing of snowmelt. A better understanding of these interactions could therefore be acquired through in situ observations of the effects of vegetation compositions on distributions of snow at the start of the snow season.

5 Conclusions

The Alternating Conditional Expectation (ACE) approach revealed non-linear associations between passive microwave derived snow water equivalent, and growing season air temperature, soil moisture and vegetation transmissivity. Although the drivers of snow accumulation vary according to the scale at which they are examined (Pomeroy et al., 2002), and uncertainty exists in passive microwave estimates of the Arctic land surface due to its heterogeneity and high lake fraction (Duguay et al., 2005; Rees et al., 2006; Green et al., 2012), it is interesting to note the similarity existing between the linkages, thresholds and associations found in situ and through ACE analysis of passive microwave observations (at 25 km).

Across all vegetation classes, sites with more aboveground biomass at the start and end of the growing season tend to have lower mean values of SWE over the first and last thirty days of the snow season. Field studies have found that snowmelt occurs more gradually over regions with more vegetation due to shading and slowed wind speeds (Metcalfe and Buttle, 1998), and that snow accumulation is diminished over regions with greater canopy density due to interception and sublimation (Pomeroy et al., 2002). The ACE technique also indicated that sites with drier soils at the end of the growing season tended to accumulate more snow at the start of the snow season. Likewise, in situ observations have indicated more rapid and thorough freezing of soils which were dry at the start of the snow season (Willis et al., 1961), which could allow snow to accumulate more easily over cooler soils.

BGD
10, 1747–1791, 2013

In forested regions, sites that tend to accumulate less snow also tend to have greater canopy density, as indicated by diminished vegetation transmissivity. Field studies have indicated that snow accumulation in heavily forested areas is limited due to canopy interception and sublimation (Church, 1933; Pomeroy et al., 2002). ACE analysis also indicated that within forested regions accumulating < 90 mm of SWE, sites with greater SWE tended to also have greater soil moisture, an observation similar to the in situ findings by Hardy et al. (2001).

In Arctic tundra regions with low (< 75 mm) SWE, more snow is accumulated at sites with warmer growing season temperatures and greater biomass or surface roughness, as indicated by diminished values of vegetation transmissivity. Arctic regions with warmer annual air temperatures have greater moisture availability for snow season precipitation (Serreze and Barry, 2005), and snow is preferentially accumulated in regions with greater vegetation or surface roughness (Walker et al., 2001). Over dry (< 0.1 soil moisture) Arctic areas, sites that have more snow at the end of the snow season tend to have wetter soils at the start of the growing season. Arctic regions that have more snow for the last thirty days of the snow season also tend to have have cooler temperatures at the start of the growing season, likely due to the rapid snowmelt undergone by cold, high latitude sites (Bonan, 2002).

Recent circumpolar predictions indicate that climate change may diminish the annual duration of snow cover and increase maximum annual SWE (Callaghan et al., 2011), and that high latitude warming and altered snow season length can affect Arctic vegetation phenology and species composition (Arft et al., 1999; Walker et al., 1999). As the ACE technique has uncovered linkages between snow and growing season land surface variables that bear great similarity to associations observed in situ, this also suggests that climate-driven changes in soil moisture, vegetation composition and air temperature may both influence, and be influenced by, shifts in the timing and accumulation of snow. We therefore suggest that continued monitoring of Arctic ecosystems at the field scale be accompanied by applying the ACE technique to monitor linkages between satellite passive microwave observations of snow and growing season variables.

BGD
10, 1747–1791, 2013

Appendix A

Data: GlobSnow SWE and NTSG land surface variables

The products compared in this study are derived from gridded Level 2A brightness temperature from the Advanced Microwave Scanning Radiometer for the Earth Observing System (AMSR-E). AMSR-E is a multichannel satellite passive microwave radiometer collecting observations at 6.925, 10.65, 18.7, 23.8 36.5 and 89.0 GHz (Kawanishi et al., 2003). Passive microwave observations rely on estimates of microwave radiance, which increases proportionally with temperature and emissivity of a surface. Brightness temperature (T_b), the variable of observation by passive microwave instruments, is a function of the product of kinetic temperature (T_k) and emissivity (ϵ): $T_b = T_k\epsilon$. T_b is equivalent to the physical temperature of a blackbody ($\epsilon = 1$) (Jones et al., 2010).

AMSR-E T_b has been used previously to estimate snow water equivalent (Kelly, 2009), vegetation and soil moisture (Njoku and Chan, 2005). These approaches have continued improving in accuracy and global coverage, culminating in the recent release of the AMSR-E derived data sets analyzed in this study: NTSG land parameters by Jones and Kimball (2012) and GlobSnow SWE by Luojus et al. (2009). The following subsections describe the methodologies applied by the Finnish Meteorological Institute (FMI) and the University of Montana's Numerical Terradynamic Simulation Group (NTSG) to calculate GlobSnow SWE and land surface variables, respectively. All data are calculated from AMSR-E brightness temperature observations acquired at 6.9, 10.7, 18.7, 23.8, 36.5 and 89.0 GHz twice daily with native resolutions varying inversely with frequency from 5 km to 60 km (Jones and Kimball, 2010a). NTSG and GlobSnow both use NSIDC Level 2A AMSR-E data, which resamples each frequency's native resolution to that of the 6.9 GHz frequency. The resulting product is on a 25 km grid (Ashcroft and Wentz, 2003) and use an EASE-Grid projection (Knowles et al., 2010). GlobSnow snow water equivalent uses 18.7 and 36.5 GHz frequency data (Luojus et al., 2009). Both the GlobSnow and AMSR-E air temperature datasets have

BGD
10, 1747–1791, 2013

been validated against in situ and AIRS/AMSU observations, respectively (Jones et al., 2010). Analysis in this study made use of AMSR-E land surface variables version 1.2 (Jones and Kimball, 2012) and version 0.9.1 of GlobSnow SWE (Luojus et al., 2009).

A1 GlobSnow snow water equivalent (winter season)

Remotely sensed retrievals of SWE are influenced by ground surface characteristics. Soil dielectric properties and soil roughness can influence SWE retrievals, but the impacts of these variables on cold dry snow SWE retrievals can be largely mitigated by estimating SWE using the difference between 18.7 and 36.5 GHz brightness temperatures (Kelly et al., 2003). SWE retrievals are highly influenced by snow grain size, which in turn, is controlled by snowpack thermal gradients. A new data set used for SWE estimates, GlobSnow, optimizes agreement between measured and simulated brightness temperature using forward simulation of different grain sizes.

GlobSnow SWE estimates (in mm) are calculated using AMSR-E 18.7 and 36.5 GHz data as well as meteorological data. Meteorological stations provide estimates of snow depth, which are filtered to remove spurious values and are then kriged between stations (Takala et al., 2011). In the GlobSnow algorithm, regions with thin snowpacks, snowmelt or wet snow are masked out, as wet snow acts as a microwave emitter (Armstrong and Brodzik, 2001). Snow grain size is estimated through an inversion of AMSR-E observations using the Helsinki University of Technology snow microwave emission model (Pulliainen et al., 1999). Snow water equivalent is then calculated from snow depth through knowledge of snow density. Single fixed variables are used to estimate snowpack, soil and forest characteristics. Surface roughness and soil moisture are assumed to have the same value across the entire pan-Arctic, and forest cover effects are removed using vegetation transmissivity collected in winter (Pulliainen, 2006). GlobSnow SWE has been validated for several northern sites, and was found to have a root mean squared error (RMSE) of 33 mm (Luojus et al., 2009).

BGD
10, 1747–1791, 2013

A2 NTSG air temperature (growing season)

The central goal in the creation of the NTSG land surface variable dataset was to gain accurate estimates of minimum and maximum air temperature (in Kelvin) at a height of 2 m using AMSR-E observations. The accuracy of NTSG air temperature estimates was improved by quantifying and removing the influence of vegetation, soil moisture and atmospheric water vapor on brightness temperature. Vegetation transmissivity and soil moisture variables were therefore extracted through this process (Jones and Kimball, 2010c).

Minimum air temperature is calculated according to morning retrievals, and maximum air temperature is calculated according to late afternoon retrievals. Both estimates carefully account for the effects of vegetation, soil moisture, fractional cover of open water on land, and atmospheric water vapor. The complete details regarding calculations of air temperature can be found in Jones et al. (2010). Air temperatures from meteorological stations were used for calibration (270 stations) and validation (273 stations) of resulting products, with these stations being assigned randomly. Comparisons indicated root mean squared error (RMSE) values of 3.5 K between AMSR-E derived temperature and meteorological data. Larger errors were observed in regions with sparse vegetation, higher elevations and higher fractional cover of open water on land. Non-desert regions had RMSE values between 1 and 3.5 K, which shows better accuracy than previous approaches that had relied on carefully selected meteorological stations (Jones et al., 2010). For the purpose of this project, daily air temperature was calculated as the daily average of maximum and minimum temperatures reported by Jones et al. (2010).

A3 NTSG soil moisture (growing season)

The emissivity of soils depends largely on its dielectric properties. The real part of the dielectric constant increases as a function of soil moisture content. As a result, wetter soils have a diminished emissivity relative to drier soils (Njoku and Kong, 1977).

BGD
10, 1747–1791, 2013

Passive microwave observations are most sensitive to subsurface soil moisture at low ($\lesssim 3$ GHz) frequencies, and at these low frequencies, the influences of vegetation and surface roughness is also limited (Njoku and Kong, 1977; Njoku and Chan, 2005).

The NTSG soil moisture product therefore relies primarily on the lowest AMSR-E frequency (6.9 GHz) to generate estimates of surface (≤ 2 cm) soil moisture (Jones and Kimball, 2010a). Soil moisture is expressed as a dimension-free value ranging between 0–1. Soil moisture was found to be correlated with precipitation at meteorological stations in the Northern Hemisphere ($0.2 < r < 0.8$) (Jones and Kimball, 2010b).

A4 NTSG vegetation transmissivity (growing season)

Vegetation acts as an attenuating layer that diminishes the transmissivity of passive microwave radiation. The vegetation water content alters the dielectric properties of the landscape, such that there exists diminished emissivity over regions with greater vegetation water content (Jackson and O'Neill, 1990). Furthermore, the vegetation canopy layers influence scattering (Jones and Kimball, 2010a), generally resulting in increased scattering and diminished transmissivity over regions that have greater biomass, although the canopy structure (stem geometry, leaf orientation, angle distributions, spatial distribution, etc.) and type of vegetation also influence the surface roughness and scattering (Njoku and Chan, 2005; Jensen, 2007). The optical depth of vegetation can thus be defined according to the height of the attenuating layer (z_{top}) and the extinction with height ($k(z)$ in m^{-1}) (Jones et al., 2010):

$$\tau = \int_0^{z_{\text{top}}} k(z)\mathrm{d}z. \tag{A1}$$

Over a vegetated region with a single species and relatively constant surface roughness, the attenuating influence of vegetation, or vegetation optical depth (τ), can be estimated as a linear function of canopy water content (g in kg m^{-2}) using a species-specific parameter (b): $\tau = b \times g$ (Jackson and O'Neill, 1990). A similar description is

BGD
10, 1747–1791, 2013

used by Jones et al. (2010) to define the optical depth of Northern Hemispheric vegetation as a function of water content using a parameter α that expresses both the influences of roughness factors (h) and look angle (θ), as well as frequency and angular impacts on canopy extinction (b in $m^2\,kg^{-1}$):

$$\tau = \alpha g = bhg\sec(\theta). \quad \text{(A2)}$$

Vegetation transmissivity to passive microwave radiation (t) can be expressed as the logarithmically scaled counterpart of vegetation optical depth: $t = \exp(-\tau)$. Vegetation transmissivity is calculated iteratively from a combination of inverted analytical expressions using AMSR-E inputs, emissivity and ratios, as detailed in Jones et al. (2010). Separate versions of the NTSG vegetation transmissivity product are available using inputs from the 6.9, 10.7 and 18.7 GHz channels. There is a great deal of similarity between these observations, and so only the 10.7 GHz channel is used in this analysis, just as in Njoku and Chan (2005).

Comparisons of this product with Moderate Resolution Imaging Spectroradiometer (MODIS) derived leaf area index, normalized difference vegetation index (NDVI) and enhanced vegetation index yielded correlations of up to 0.9 (Jones et al., 2011). As the aforementioned MODIS products are typically used to estimate the vegetation health or quantity of aboveground biomass, it seems reasonable to assume that vegetation transmissivity likewise provides a relatively reliable estimate of the quantity of aboveground biomass.

Acknowledgements. The authors would like to thank John Kimball and Lucas Jones (NTSG), and Jouni Pulliainen and Kari Luojus (FMI) for allowing public access to the AMSR-E Land Surface Parameter and GlobSnow Snow Water Equivalent data sets.

BGD
10, 1747–1791, 2013

References

Adams, J., Bond, N., and Overland, J.: Regional variability of the Arctic heat budget in fall and winter, J. Climate, 13, 3500–3510, 2000. 1759

Arft, A., Walker, M., Gurevitch, J., Alatalo, J., Bret-Harte, M., Dale, M., Diemer, M., Gugerli, F., Henry, G., Jones, M., Hollister, R., Jónsdóttir, I., Laine, K., Lévesque, E., Marion, G., Molau, U., Mølgaard, P., Nordenhäll, U., Raszhivin, V., Robinson, C., Starr, G., Stenström, A., Stenström, M., Totland, Ø., Turner, P., Walker, L., Webber, P., Welker, J., and Wookey, P.: Responses of tundra plants to experimental warming: meta-analysis of the international tundra experiment, Ecol. Monogr., 69, 491–511, 1999. 1769

Armstrong, R. and Brodzik, M.: Recent Northern Hemisphere snow extent: a comparison of data derived from visible and microwave satellite sensors, Geophys. Res. Lett., 28, 3673–3676, 2001. 1771

Ashcroft, P. and Wentz, F.: AMSR-E/Aqua L2A Global Swath Spatially-Resampled Brightness Temperatures (Tb) V001, digital media, National Snow and Ice Data Center, Boulder, CO, 2003. 1770

Ayres, E., Nkem, J., Wall, D., Adams, B., Barrett, J., Simmons, B., Virginia, R., and Fountain, A.: Experimentally increased snow accumulation alters soil moisture and animal community structure in a polar desert, Polar Biol., 33, 897–907, 2010. 1761

Bonan, G.: Ecological Climatology: Concepts and Applications, Cambridge Univ. Press, 2002. 1759, 1760, 1769

Breiman, L. and Friedman, J.: Estimating optimal transformations for multiple regression and correlation, J. Am. Stat. Assoc., 80, 580–598, 1985. 1751, 1752

Burt, T. and Butcher, D.: Topographic controls of soil moisture distributions, Eur. J. Soil Sci., 36, 469–486, 1985. 1761

Callaghan, T., Johansson, M., Brown, R., Groisman, P., Labba, N., Radionov, V., Barry, R., Bulygina, O., Essery, R., Frolov, D., Golubev, V., Grenfell, T., Petrushina, M., Razuvaev, V., Robinson, D., Romanov, P., Shindell, D., Shmakin, A., Sokratov, S., Warren, S., and Yang, D.: The changing face of Arctic snow cover: a synthesis of observed and projected changes, AMBIO, 40, 17–31, 2011. 1756, 1769

Church, J.: Snow surveying: its principles and possibilities, Geogr. Rev., 23, 529–563, 1933. 1766, 1769

D'Agostino, R. and Stephens, M.: Goodness-of-fit Techniques, vol. 68, CRC, 1986. 1757

BGD
10, 1747–1791, 2013

Duguay, C., Green, J., Derksen, C., English, M., Rees, A., Sturm, M., and Walker, A.: Preliminary assessment of the impact of lakes on passive microwave snow retrieval algorithms in the Arctic, in: 62nd Eastern Snow Conference Proceedings, 2005. 1768
Essery, R. and Pomeroy, J.: Vegetation and topographic control of wind-blown snow distributions in distributed and aggregated simulations for an arctic tundra basin, J. Hydrometeorol., 5, 735–744, 2004. 1765
Evans, B., Walker, D., Benson, C., Nordstrand, E., and Petersen, G.: Spatial interrelationships between terrain, snow distribution and vegetation patterns at an arctic foothills site in Alaska, Ecography, 12, 270–278, 1989. 1765
Fitzgibbon, J. and Dunne, T.: Characteristics of subarctic snowcover/Les caractéristiques de la couverture de neige presque arctique, Hydrolog. Sci. J., 24, 465–476, 1979. 1765
Frank, I. and Lanteri, S.: ACE: a non-linear regression model, Chemometr. Intell. Lab., 3, 301–313, 1988. 1751, 1752
French, H. and Binley, A.: Snowmelt infiltration: monitoring temporal and spatial variability using time-lapse electrical resistivity, J. Hydrol., 297, 174–186, 2004. 1761
Gatswirth, J., Gel, Y., and Miao, W.: The impact of Levene's test of equality of variances on statistical theory and practice, Stat. Sci., 24, 343–360, 2009. 1756
Gel, Y.: Comparative analysis of the local observation-based (LOB) method and the nonparametric regression-based method for gridded bias correction in mesoscale weather forecasting, Weather Forecast., 22, 1243–1256, 2007. 1751
Gelfan, A., Pomeroy, J., and Kuchment, L.: Modeling forest cover influences on snow accumulation, sublimation, and melt, J. Hydrometeorol., 5, 785–803, 2004. 1766, 1767
Golding, D. and Swanson, R.: Snow distribution patterns in clearings and adjacent forest, Water Resour. Res., 22, 1931–1940, 1986. 1766
Green, J., Kongoli, C., Prakash, A., Sturm, M., Duguay, C., and Li, S.: Quantifying the relationships between lake fraction, snow water equivalent and snow depth, and microwave brightness temperatures in an arctic tundra landscape, Remote Sens. Environ., 127, 329–340, 2012. 1768
Grippa, M., Kergoat, L., Toan, T. L., Mognard, N., Delbart, N., L'Hermitte, J., and Vicente-Serrano, S.: The impact of snow depth and snowmelt on the vegetation variability over central Siberia, Geophys. Res. Lett., 32, L21412, doi:10.1029/2005GL024286, 2005. 1765
Hardy, J., Groffman, P., Fitzhugh, R., Henry, K., Welman, A., Demers, J., Fahey, T., Driscoll, C., Tierney, G., and Nolan, S.: Snow depth manipulation and its influence on soil frost and water

BGD
10, 1747–1791, 2013

dynamics in a northern hardwood forest, Biogeochemistry, 56, 151–174, 2001. 1761, 1763, 1769
Hare, F.: The Arctic, Q. J. Roy. Meteor. Soc., 94, 439–459, 1968. 1756
Jackson, T. and O'Neill, P.: Attenuation of soil microwave emission by corn and soybeans at 1.4 and 5 GHz, IEEE T. Geosci. Remote, 28, 978–980, 1990. 1773
Janowicz, R., Gray, D., and Pomeroy, J.: Spatial variability of fall soil moisture and spring snow water equivalent within a mountainous sub-arctic watershed, in: Proceedings of the Eastern Snow Conference, vol. 60, 127–139, 2003. 1761
Jensen, J. R.: Remote Sensing of the Environment: An Earth Resource Perspective, 2nd edn., Pearson Prentice Hall, 2007. 1765, 1773
Johnsson, H. and Lundin, L.-C.: Surface runoff and soil water percolation as affected by snow and soil frost, J. Hydrol., 122, 141–159, 1991. 1761, 1763
Jones, L. and Kimball, J.: A global daily record of land surface parameter retrievals from AMSR-E Version 1.1, 2010a. 1770, 1773
Jones, L. and Kimball, J.: Daily Global Land Surface Parameters Derived from AMSR-E, available at: http://nsidc.org/data/docs/daac/nsidc0451_amsre_derived_land_params/pdfs/nsidc0451_amsre_land_parameters.pdf, 2010b. 1773
Jones, L. A. and Kimball, J. S.: Daily Global Land Surface Parameters Derived from AMSR-E, digital media, 2010c. 1772
Jones, L. and Kimball, J.: Daily Global Land Surface Parameters Derived from AMSR-E, digital media, National Snow and Ice Data Center, Boulder, Colorado, USA, 2012. 1750, 1770, 1771
Jones, L., Ferguson, C., Kimball, J., Zhang, K., Chan, S., McDonald, K., Njoku, E., and Wood, E.: Satellite microwave remote sensing of daily land surface air temperature minima and maxima from AMSR-E, IEEE J. Sel. Top. Appl., 3, 111–123, 2010. 1766, 1770, 1771, 1772, 1773, 1774
Jones, M., Kimball, J., McDonald, K., and Jones, L.: Utilizing satellite passive microwave remote sensing for monitoring global land surface phenology, Remote Sens. Environ., 115, 1102–1114, 2011. 1774
Jung, M., Henkel, K., Herold, M., and Churkina, G.: Exploiting synergies of global land cover products for carbon cycle modeling, Remote Sens. Environ., 101, 534–553, 2006. 1755

BGD
10, 1747–1791, 2013

Kane, D., Hinzman, L., Benson, C., and Liston, G.: Snow hydrology of a headwater arctic basin 1. Physical measurements and process studies, Water Resour. Res., 27, 1099–1109, 1991. 1763

Kawanishi, T., Sezai, T., Ito, Y., Imaoka, K., Takeshima, T., Ishido, Y., Shibata, A., Miura, M., Inahata, H., and Spencer, R.: The Advanced Microwave Scanning Radiometer for the Earth Observing System (AMSR-E), NASDA's contribution to the EOS for global energy and water cycle studies, IEEE T. Geosci. Remote, 41, 184–194, 2003. 1770

Kelly, R.: The AMSR-E snow depth algorithm: description and initial results, J. Remote Sens. Soc. Jpn., 29, 307–317, 2009. 1770

Kelly, R., Chang, A., Tsang, L., and Foster, J.: A prototype AMSR-E global snow area and snow depth algorithm, IEEE T. Geosci. Remote, 41, 230–242, 2003. 1771

Knowles, K., Savoie, M., Armstrong, R., and Brodzik, M.: AMSR-E/Aqua daily EASE grid brightness temperatures, available at: http://nsidc.org/data/nsidc-0301.html, NSIDC, 2010. 1770

Levene, H.: Robust testes for equality of variances, in: Contributions to Probability and Statistics, Stanford University Press, 1960. 1755

Liston, G. and Sturm, M.: Winter precipitation patterns in arctic Alaska determined from a blowing-snow model and snow-depth observations, J. Hydrometeorol., 3, 646–659, 2002. 1766

Lundberg, A. and Halldin, S.: Snow interception evaporation. Review of measurementtechniques, processes, and models, Theor. Appl. Climatol., 70, 117–133, 2001. 1766, 1767

Luojus, K., Pulliainen, J., and Derksen, C.: Snow Water Equivalent (SWE) Product Guide, Global Snow Monitoring for Climate Research, 0.9.1/01, 2009. 1750, 1770, 1771

MacDonald, M., Pomeroy, J., and Pietroniro, A.: Parameterizing redistribution and sublimation of blowing snow for hydrological models: tests in a mountainous subarctic catchment, Hydrol. Process., 23, 2570–2583, 2009. 1766

Metcalfe, R. and Buttle, J.: A statistical model of spatially distributed snowmelt rates in a boreal forest basin, Hydrol. Process., 12, 1701–1722, 1998. 1767, 1768

Njoku, E. and Chan, S.: Vegetation and surface roughness effects on AMSR-E land observations, Remote Sens. Environ., 100, 190–199, 2005. 1766, 1770, 1773, 1774

Njoku, E. and Kong, J.: Theory for passive microwave remote sensing of near-surface soil moisture, J. Geophys. Res., 82, 3108–3118, 1977. 1772, 1773

BGD
10, 1747–1791, 2013

Nowinski, N., Taneva, L., Trumbore, S., and Welker, J.: Decomposition of old organic matter as a result of deeper active layers in a snow depth manipulation experiment, Oecologia, 163, 785–792, 2010. 1765

Overland, J., Adams, J., and Bond, N.: Regional variation of winter temperatures in the Arctic, J. Climate, 10, 821–837, 1997. 1759

Pomeroy, J., March, P., Jones, H., and Davies, T.: chap. Spatial distribution of snow chemical load at the tundra-taiga transition, in: Biogeochemistry of Seasonally Snow-Covered Catchments, IAHS, 191–206, 1995. 1766

Pomeroy, J., Granger, R., Pietroniro, A., Elliott, J., Toth, B., and Hedstrom, N.: Hydrological Pathways in the Prince Albert Model Forest, Tech. rep., National Hydrology Research Institute Environment Canada, Saskatoon, Saskatchewan, 1997. 1766, 1767

Pomeroy, J., Gray, D., Shook, K., Toth, B., Essery, R., Pietroniro, A., and Hedstrom, N.: An evaluation of snow accumulation and ablation processes for land surface modelling, Hydrol. Process., 12, 2339–2367, 1999. 1767

Pomeroy, J., Gray, D., Hedstrom, N., and Janowicz, J.: Prediction of seasonal snow accumulation in cold climate forests, Hydrol. Process., 16, 3543–3558, 2002. 1749, 1767, 1768, 1769

Pomeroy, J., Bewley, D., Essery, R., Hedstrom, N., Link, T., Granger, R., Sicart, J., Ellis, C., and Janowicz, J.: Shrub tundra snowmelt, Hydrol. Process., 20, 923–941, 2006. 1766

Prince, S. and Goward, S.: Global primary production: a remote sensing approach, J. Biogeogr., 22, 815–835, 1995. 1756

Pulliainen, J.: Mapping of snow water equivalent and snow depth in boreal and sub-arctic zones by assimilating space-borne microwave radiometer data and ground-based observations, Remote Sens. Environ., 101, 257–269, 2006. 1771

Pulliainen, J., Grandell, J., and Hallikainen, M.: HUT snow emission model and its applicability to snow water equivalent retrieval, IEEE T. Geosci. Remote, 37, 1378–1390, 1999. 1771

Rees, A., Derksen, C., English, M., Walker, A., and Duguay, C.: Uncertainty in snow mass retrievals from satellite passive microwave data in lake-rich high-latitude environments, Hydrol. Process., 20, 1019–1022, 2006. 1768

Rigor, I., Colony, R., and Martin, S.: Variations in surface air temperature in the Arctic, J. Climate, 13, 896–914, 2000. 1759

Ritchie, J. and Hare, F.: Late-quaternary vegetation and climate near the arctic treeline of northwestern North America, Quaternary Res., 1, 331–342, 1971. 1756

BGD
10, 1747–1791, 2013

Rouse, W.: Soil microclimate of tundra and forest, Water Resour. Res., 20, 67–73, 1984. 1760
Serreze, M. and Barry, R.: The Arctic Climate System, Cambridge Univ. Press, 2005. 1749, 1756, 1759, 1761, 1769
Shinoda, M.: Climate memory of snow mass as soil moisture over central Eurasia, J. Geophys. Res., 106, 33393–33403, 2001. 1749, 1762
Sitch, S., McGuire, A. D., Kimball, J., Gedney, N., Gamon, J., Engstrom, R., Wolf, A., Zhuang, Q., Clein, J., and McDonald, K. C.: Assessing the carbon balance of circumpolar Arctic tundra using remote sensing and process modeling, Ecol. Appl., 17, 213–234, 2007. 1749
Smith, K., Gholz, H. L., and de Assis Oliveira, F.: Litterfall and nitrogen-use efficiency of plantations and primary forest in the eastern Brazilian Amazon, Forest Ecol. Manag., 109, 209–220, doi:10.1016/S0378-1127(98)00247-3, 1998. 1760
Staple, W., Lehane, J., and Wenhardt, A.: Conservation of soil moisture from fall and winter precipitation, Can. J. Soil Sci., 40, 80–88, 1960. 1763
Sturm, M., Holmgren, J., and Liston, G.: A seasonal snow cover classification system for local to global applications, J. Climate, 8, 1261–1283, 1995. 1749
Sturm, M., Holmgren, J., McFadden, J., Liston, G., Chapin III, F., and Racine, C.: Snow-shrub interactions in Arctic Tundra: a hypothesis with climatic implications, J. Climate, 14, 336–344, 2001a. 1749, 1765, 1766
Sturm, M., Pielke Sr, R., and Chapin III, F.: Interactions of shrubs and snow in arctic tundra: measurements and models, in: Soil-Vegetation-Atmosphere Transfer Schemes and Large-Scale Hydrological Models, Proceedings of an International Symposium (Symposium S5) held during the Sixth Scientific Assembly of the International Association of Hydrological Sciences (IAHS) at Maastricht, The Netherlands, from 18 to 27 July 2001, vol. 270, 317, International Assn of Hydrological Sciences, 2001b. 1766
Sturm, M., Douglas, T., Racine, C., and Liston, G.: Changing snow and shrub conditions affect albedo with global implications, J. Geophys. Res., 110, G01004, doi:10.1029/2005JG000013, 2005. 1767
Suzuki, K., Kubota, J., Ohata, T., and Vuglinsky, V.: Influence of snow ablation and frozen ground on spring runoff generation in the Mogot Experimental Watershed, southern mountainous taiga of eastern Siberia, Nord. Hydrol., 37, 21–29, 2006. 1763
Takala, M., Luojus, K., Pulliainen, J., Derksen, C., Lemmetyinen, J., Kärnä, J., Koskinen, J., and Bojkov, B.: Estimating Northern Hemisphere snow water equivalent for climate research

BGD
10, 1747–1791, 2013

through assimilation of space-borne radiometer data and ground-based measurements, Remote Sens. Environ., 115, 3517–3529, 2011. 1771
Tranquillini, W.: The physiology of plants at high altitudes, Ann. Rev. Plant Physio., 15, 345–362, 1964. 1765
Wahren, C., Walker, M., and Bret-Harte, M.: Vegetation responses in Alaskan arctic tundra after 8 years of a summer warming and winter snow manipulation experiment, Glob. Change Biol., 11, 537–552, 2005. 1749
Walker, D., Billings, W., and De Molenaar, J.: Snow–vegetation interactions in tundra environments, in: Snow Ecology: an Interdisciplinary Examination of Snow-Covered Ecosystems, 266–324, 2001. 1765, 1769
Walker, D., Raynolds, M., Daniëls, F., Einarsson, E., Elvebakk, A., Gould, W., Katenin, A., Kholod, S., Markon, C., Melnikov, E., Moskalenko, N., Talbot, S., Yurtsev, B., Bliss, L., Edlund, S., Zoltai, S., Wilhelm, M., Bay, C., Gudjónsson, G., Ananjeva, G., Drozdov, D., Konchenko, L., Korostelev, Y., Ponomareva, O., Matveyeva, N., Safranova, I., Shelkunova, R., Polezhaev, A., Johansen, B., Maier, H., Murray, D., Fleming, M., Trahan, N., Charron, T., Lauritzen, S., and Vairin, B.: The Circumpolar Arctic vegetation map, J. Veg. Sci., 16, 267–282, 2005. 1755
Walker, M., Walker, D., Welker, J., Arft, A., Bardsley, T., Brooks, P., Fahnestock, J., Jones, M., Losleben, M., Parsons, A., Seastedt, T., and Turner, P.: Long-term experimental manipulation of winter snow regime and summer temperature in arctic and alpine tundra, Hydrol. Process., 13, 2315–2330, 1999. 1769
Wardle, P.: Engelmann spruce (*Picea engelmannii* Engel.) at its upper limits on the Front Range, Colorado, Ecology, 49, 483–495, 1968. 1765
Williams, M. and Ratsetter, E.: Vegetation characteristics and primary productivity along an arctic transect: implications for scaling-up, J. Ecol., 87, 885–898, 1999. 1761
Willis, W., Carlson, C., Alessi, J., and Haas, H.: Depth of freezing and spring run-off as related to fall soil-moisture level, Can. J. Soil Sci., 41, 115–123, 1961. 1763, 1764, 1768
Zhao, L. and Gray, D.: Estimating snowmelt infiltration into frozen soils, Hydrol. Process., 13, 1827–1842, 1999. 1763, 1764

BGD
10, 1747–1791, 2013

Table 1. Aggregation of forest SYNMAP and CAVM vegetation classes into a categorization that divides the pan-Arctic into seven broad vegetation classes: evergreen forest (EVGRN), deciduous forest (DECDS), mixed forest containing shrubs or grasses (MFRST), shrub dominated region (SHRUB), graminoid tundra (GRMTD), shrub tundra (SRBTD), barren vegetated region (BARRN). Regions of water or permanent snow and ice (MASKD) are excluded from the analysis.

Veg class	Source	Description
EVGRN	SYNMAP	Trees needle evergreen; trees broad evergreen; trees mixed evergreen
DECDS	SYNMAP	Trees needle deciduous; trees needle mixed; trees broad deciduous; Trees broad mixed; trees mixed deciduous; trees mixed mixed
MFRST	SYNMAP	Trees and shrubs; trees and grasses; trees and crops; crops
SHRUBS	SYNMAP	Shrubs; shrubs and crops
SRBTD	SYNMAP	Shrubs and barren
SRBTD	CAVM	Prostrate dwarf-shrub, herb tundra; erect dwarf-shrub tundra; Low-shrub tundra
GRMTD	SYNMAP	Grasses; grasses and crops
GRMTD	CAVM	Rush/grass, forb, cryptogam tundra; graminoid, prostrate dwarf-shrub, forb tundra; Prostrate/hemiprostrate dwarf-shrub tundra; nontussock sedge, dwarf-shrub, moss tundra; tussock-sedge, dwarf-shrub, moss tundra
BARRN	SYNMAP	Grasses and barren; barren
BARRN	CAVM	Cryptogam, herb barren; cryptogam barren complex (bedrock); Sedge/grass, moss wetland; sedge, moss, dwarf-shrub wetland; Sedge, moss, low-shrub wetland; noncarbonate mountain complex; Carbonate mountain complex
MASKD	SYNMAP	Urban; Snow and ice
MASKD	CAVM	Nunatak complex; glaciers; water; lagoon

BGD
10, 1747–1791, 2013

Table 2. Results from Levene's test examining homogeneity of variances of all variables within seven vegetation classes (Table 1), and a class containing permanent snow and ice which is masked from analysis (MASKD). These variables are air temperature (TA), volumetric soil moisture (MV), vegetation transmissivity at 10 GHz (TC10), snow water equivalent (SWE) and net primary productivity (NPP). All p-values are $< 10^{-5}$.

	TA	MV	TC10	SWE	NPP
EVGRN	2.52	1.06×10^{-3}	4.26×10^{-3}	898	9.05×10^{3}
DECDS	1.92	9.25×10^{-4}	3.76×10^{-3}	556	6.84×10^{3}
MFRST	1.77	8.35×10^{-4}	3.23×10^{-3}	620	1.04×10^{4}
SHRUB	2.46	8.27×10^{-4}	4.76×10^{-3}	675	1.30×10^{4}
GRMTD	5.77	6.71×10^{-4}	1.13×10^{-2}	790	2.28×10^{4}
SRBTD	4.73	4.90×10^{-4}	1.03×10^{-2}	437	2.55×10^{4}
BARRN	6.21	6.67×10^{-4}	1.20×10^{-2}	327	3.03×10^{4}
MASKD	6.52	5.56×10^{-4}	8.71×10^{-3}	279	2.77×10^{4}
Test statistic	48.4	24.5	67.1	22.3	105

BGD
10, 1747–1791, 2013

Table 3. R^2 values from the linear regressions of SWE and air temperature (TA), SWE and volumetric soil moisture (MV), and of SWE and vegetation transmissivity at 10.7 GHz (TC). Comparisons of SWE and growing season observations were conducted by comparing mean annual 2003–2008 values (mean), and by examining associations between SWE at the end of the snow season with growing season variables at the start of the growing season (spring), and between growing season variables at the end of the growing season with SWE at the start of the snow season (autumn). R^2 values in single linear regression that correspond to a p-value > 0.01 are marked with an asterisk.

Var	Time	EVGRN	DECDS	MFRST	SHRUB	GRMTD	SRBTD	BARRN
TA	Annual	0.00	0.01	0.00*	0.02	0.11	0.04	0.20
TA	Spring	0.06	0.01	0.13	0.14	0.16	0.14	0.10
TA	Autumn	0.13	0.12	0.22	0.13	0.06	0.10	0.06
MV	Annual	0.02	0.01	0.01	0.02	0.010	0.02	0.00*
MV	Spring	0.01	0.00*	0.00	0.00*	0.00*	0.00*	0.00
MV	Autumn	0.05	0.06	0.01	0.01	0.00	0.00	0.00
TC	Annual	0.05	0.02	0.02	0.17	0.06	0.05	0.15
TC	Spring	0.20	0.11	0.23	0.28	0.20	0.19	0.18
TC	Autumn	0.16	0.28	0.22	0.16	0.02	0.06	0.03
(TA,	Annual	0.09	0.07	0.07	0.23	0.15	0.07	0.26
MV,	Spring	0.01	0.01	0.00	0.01	0.08	0.06	0.14
TC)	Autumn	0.13	0.11	0.08	0.12	0.04	0.02	0.08

BGD
10, 1747–1791, 2013

Table 4. R^2 values from the multiple linear regression of SWE vs factor scores obtained from the principal component analysis (PCA) of TA, MV, and TC. The retained principal components (PC) are determined based on the proportion of explained variance, i.e. only PC accounting for > 10 % of the total variance are included.

Time	EVGRN	DECDS	MFRST	SHRUB	GRMTD	SRBTD	BARRN
Annual	0.03	0.05	0.07	0.10	0.11	0.07	0.24
Spring	0.01	0.01	0.00	0.01	0.08	0.06	0.14
Autumn	0.13	0.11	0.08	0.12	0.04	0.02	0.08

BGD
10, 1747–1791, 2013

Table 5. R^2 values of ACE transformed SWE and ACE transformed air temperature (TA), volumetric soil moisture (MV) and vegetation canopy transmissivity (TC). Linkages are indicated using observations collected over three non-overlapping time periods of the snow and growing seasons. Associations are therefore indicated between mean annual values of SWE and growing season values, and between mean SWE 30 days prior to snowmelt and growing season values 30 days following full snowmelt (Spring), and vice versa (Autumn). In the multivariate case, the p-values of all coefficients are statistically significant. All p-values corresponding to the pair-wise ACE transformations are $< 10^{-5}$.

Var	Time	EVGRN	DECDS	MFRST	SHRUB	GRMTD	SRBTD	BARRN
TA	Annual	0.08	0.04	0.06	0.04	0.33	0.20	0.38
TA	Spring	0.09	0.04	0.15	0.16	0.17	0.15	0.12
TA	Autumn	0.16	0.14	0.25	0.17	0.07	0.10	0.06
MV	Annual	0.05	0.07	0.05	0.05	0.03	0.02	0.09
MV	Spring	0.04	0.02	0.03	0.17	0.08	0.06	0.05
MV	Autumn	0.06	0.12	0.10	0.08	0.09	0.06	0.07
TC	Annual	0.10	0.03	0.12	0.26	0.25	0.19	0.29
TC	Spring	0.22	0.19	0.24	0.31	0.21	0.22	0.19
TC	Autumn	0.17	0.30	0.27	0.19	0.04	0.09	0.06
(TA,	Annual	0.20	0.33	0.13	0.34	0.37	0.29	0.47
MV,	Spring	0.07	0.14	0.02	0.06	0.17	0.11	0.19
TC)	Autumn	0.16	0.13	0.11	0.17	0.10	0.07	0.12

BGD
10, 1747–1791, 2013

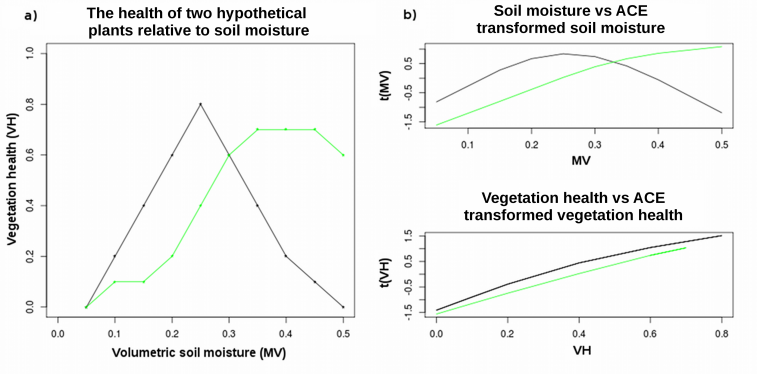

Fig. 1. Simple example illustrating the application of the ACE algorithm to hypothetical input data (**a** – x vs. y), and the resulting point pair output (**b** – top:$[x, f(x)]$; bottom:$[y, g(y)]$).

BGD
10, 1747–1791, 2013

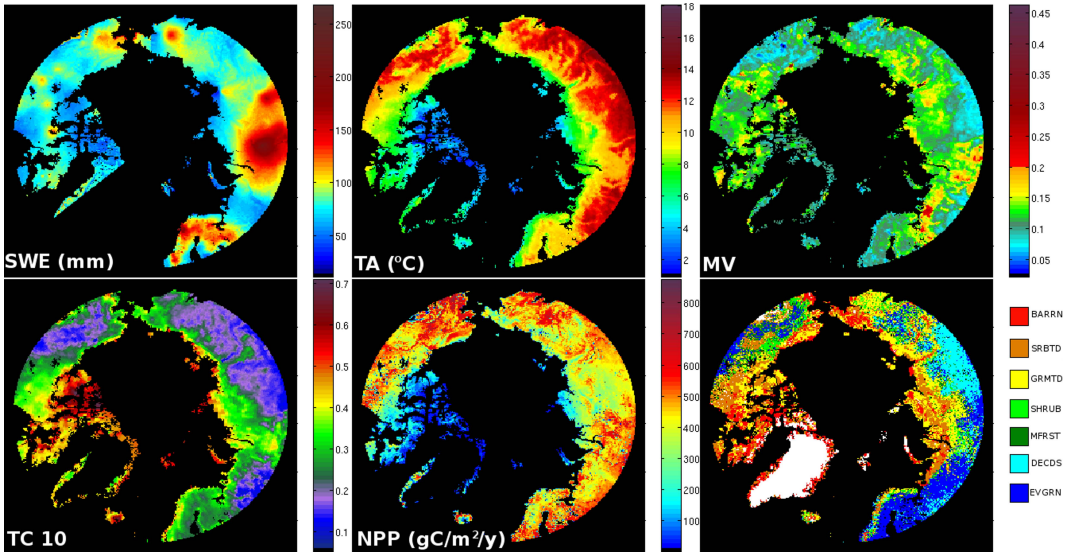

Fig. 2. Pan-Arctic (north of 60°): **(a)** mean 2003–2008 snow season GlobSnow snow water equivalent (SWE); **(b–d)** mean 2003–2008 NTSG growing season air temperature (TA), volumetric soil moisture at 2 cm (MV), and vegetation transmissivity at 10 GHz (TC10); **(e)** 1982–2000 mean GloPEM net primary productivity (NPP); and **(f)** vegetation classes used in this study, as described in Table 1.

BGD
10, 1747–1791, 2013

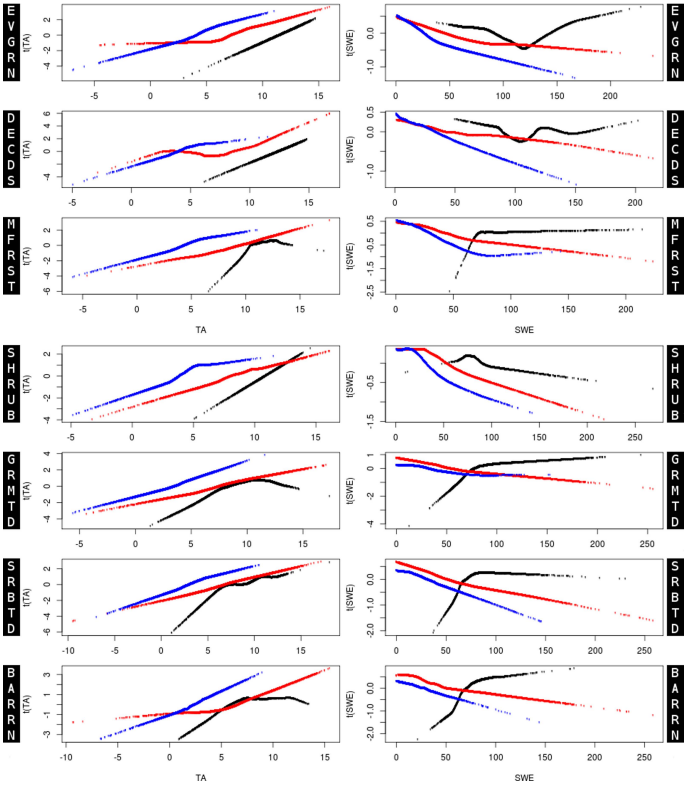

Fig. 3. Point pair output from the ACE algorithm indicating associations between air temperature (TA) and SWE ([TA,t(TA)] and [SWE,t(SWE)]) over three time periods: mean annual (black), 30 days preceding and 30 days following snowmelt (red), and 30 days preceding and 30 days following snow onset (blue). Results are indicated for all seven vegetation classes separately.

BGD
10, 1747–1791, 2013

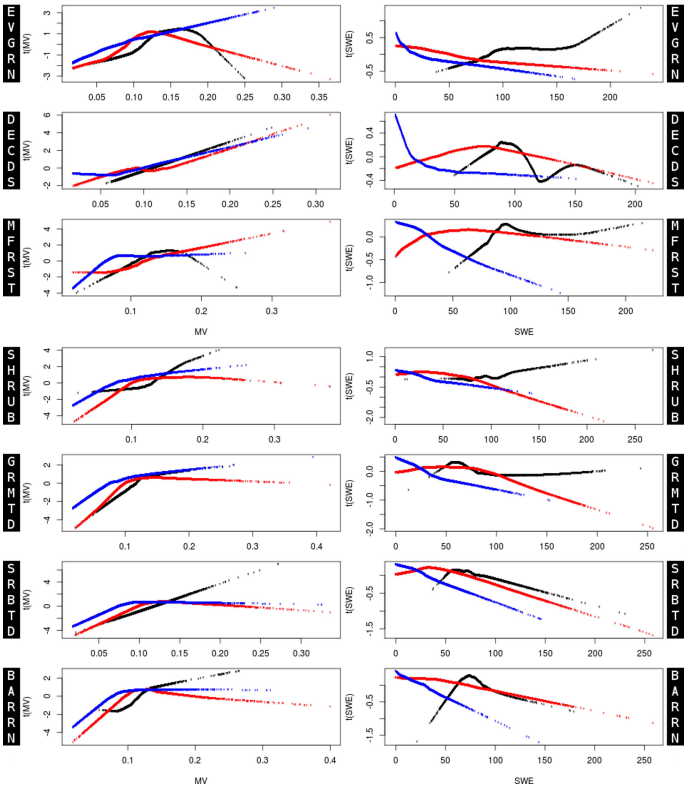

Fig. 4. Linkages between SWE and volumetric soil moisture (MV), as indicated by the optimal transformations identified using the ACE approach. The point pairs [MV,t(MV)] and [SWE,t(SWE)] were independently calculated for each vegetation class. Associations between mean 2003–2008 values are shown in black, and associations in "spring" and "autumn" are shown in red and blue.

BGD
10, 1747–1791, 2013

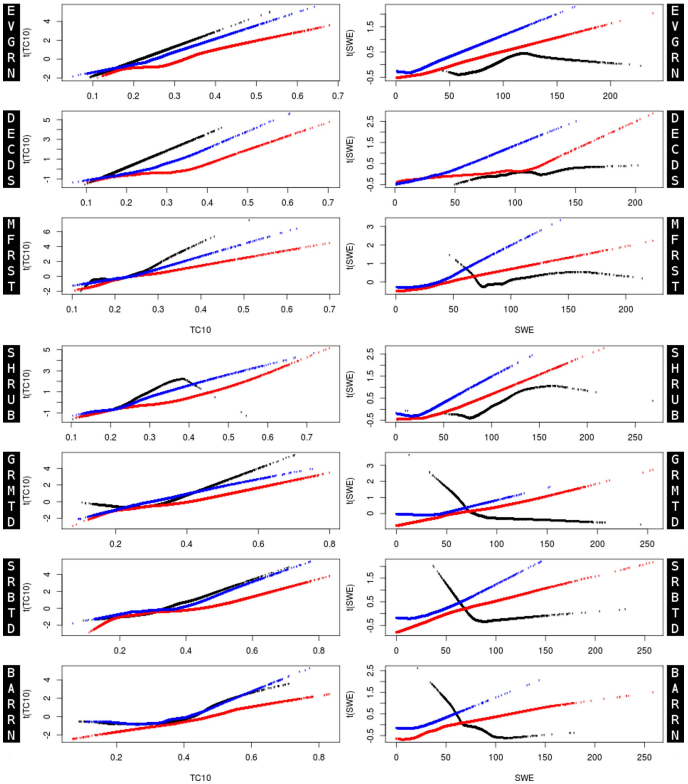

Fig. 5. Associations between satellite estimates of vegetation transmissivity at 10 GHz (TC10) and SWE over seven vegetation classes, and three time periods: mean 2003–2008 (black), before and after snowmelt (red), and preceding and following snow onset (blue). Each plot indicates the point pairs [TC10,t(TC10)] and [SWE,t(SWE)] identified using the ACE technique.

BGD
10, 1747–1791, 2013